Estimation of the Hydrodynamics Coefficients of an ROV using Free Decay Pendulum Motion

Eng YH, Lau WS, Low E., Seet GGL and CS Chin

Abstract—**A good dynamics model is essential and critical for the successful design of navigation and control system of an underwater vehicle. However, it is difficult to determine the hydro-dynamics forces, especially the added mass and the drag coefficients. In this paper, a new experimental method has been used to find the hydrodynamics forces for the ROV II, a remotely operated underwater vehicle. The proposed method is based on the classical free decay test, but with the spring oscillation replaced by a pendulum motion. The experiment results determined from the free decay test of a scaled model compared well with the simulation results obtained from well-established computational fluid dynamics (CFD) program. Thus, the proposed approach can be used to find the added mass and drag coefficients for other underwater vehicles.**

Index Terms—**Free Decay Test, Hydrodynamics Coefficients, Modeling, System Identification, Underwater Vehicles**

I. Introduction

In the recent past, Unmanned Underwater Vehicles (UUVs) have been used to explore the secrets of the oceans and to mine deep sea resources. Generally, UUVs can be classified as Remotely Operated Vehicles (ROVs) and Autonomous Underwater Vehicles (AUVs). Between the two, the ROV is the main workhorse used in the industry. Compare to a human diver, an ROV can go deeper and into riskier areas. Furthermore, it can carry out a vast variety of tasks such as underwater inspections, scientific and environmental data acquisition, construction, maintenance as well as repair of benthic stations. In essence, the use of underwater robotic system will greatly benefit all kinds of ocean activities [1].

Manuscript received July 13, 2008.

Eng YH is with the Robotic Research Center, School of Mechanical & Aerospace Engineering (MAE), Nanyang Technological University, 50 Nanyang Ave, 639798 Singapore (phone: 606-790-5568; fax: 606-793-5921; e-mail: L060006@ ntu.edu.sg).

Lau WS is with the School of Mechanical & Aerospace Engineering (MAE), Nanyang Technological University, 50 Nanyang Ave, 639798 (e-mail: mwslau@ntu.edu.sg).

Low E. is with the School of Mechanical & Aerospace Engineering (MAE), Nanyang Technological University, 50 Nanyang Ave, 639798 (e-mail: melow@ntu.edu.sg).

Seet GGL is with the School of Mechanical & Aerospace Engineering (MAE), Nanyang Technological University, 50 Nanyang Ave, 639798 (e-mail: mglseet@ntu.edu.sg).

CS Chin is with the School of Mechanical & Aerospace Engineering (MAE), Nanyang Technological University, 50 Nanyang Ave, 639798 (e-mail: chin0014@ntu.edu.sg).

A dynamics model is essential in the design of guidance, navigation and control (GNC) systems of an underwater vehicle. This has been described in Caccia [2] where the need for performance improvements in GNC has motivated deeper investigation into hydrodynamics modeling and the identification of the open frame ROV dynamics.

However, the identification of hydrodynamics parameters is very difficult and challenging. As indicated by Alessandri [3], it is difficult to tune an accurate and complete dynamics model for an ROV mainly because of the hydrodynamics parameters. In particular, the hovering and tight maneuvering motions of an underwater vehicle is difficult to characterize hydro-dynamically [4].

According to Conte [5], the greatest problem encountered in designing an efficient automatic controller is the difficulty in knowing the value of the hydrodynamics parameters with sufficient accuracy.

A wide variety of methods to identify the hydrodynamics parameters have been proposed. Traditionally, the hydrodynamics coefficients are identified through tow tank tests of the vehicle itself or of its scaled model [6, 7]. Special equipment called planar motion mechanism (PMM) is built above the tow tank to move the vehicle in a planar motion. Subsequently, the hydrodynamics coefficients are obtained using system identification techniques. Since the measured forces and moments are available in six degree of freedoms (DOF), the tow tank test allows complete model identification. However, building the tow tank that equipped a PMM is very costly. In addition, the test procedures are highly time-consuming.

More recently, the use of on-board sensor-based identification has become popular as reported in [3, 8, 9]. This technique is preferable because it makes use of on-board sensors and thrusters in the process of identification. No other equipment is needed. The technique is cost effective and the repeatability is high. It is very suitable for variable configuration ROV where payload and shape of ROV may change according to different missions [2]. However, most of the works simplify the model to an uncoupled one DOF model, which needs the motion of the ROV to be constrained to a single DOF during identification. This is hard to implement in practice. In addition, it is also hard to model the thruster forces and to measure the vehicle's responses accurately.

The use of free decay test in finding the hydrodynamics coefficients was reported by Morrison [4] in 1993. In his study, the hydrodynamics coefficients of the *ROV Hylas* were determined successfully for the heave motion. The ROV Hylas was allowed to oscillate in water by hanging it from an overhead crane by using three springs. The position of the Hylas was determined using Sonic High Accuracy Ranging and Positioning System (SHARPS). Free decay test have also been studied by Andrew [10] to identify a multiple-DOF model of an UUV. In his proposed experiment, the underwater vehicle is attached to four springs. The method was tested using a computer simulation and the results converge to true values. The proposed free decay tests exhibit a few problems in practice. Firstly, the vehicle's positions are needed during identification and the main problem is the ability to measure the vehicle states accurately. In Morrison [4], this problem is solved by employing an expensive underwater positioning system (SHARPS). In Andrew [10], only computer simulation is done. Secondly, all the springs must always be kept in tension during the oscillations. It is challenging for such experiment configuration to constraint the ROV motion within the predefined DOF. As a result, the mathematical model may not represent the motion accurately and thus the identified results might be poor.

In this paper, the hydrodynamics added mass and drag forces will be determined experimentally using a scaled down model (called the scaled model, Fig 1) of the ROV II (called the real model). The scaled model is set to oscillate in water when it is displaced from its equilibrium position and due to the hydrodynamics forces that resist the motion, the amplitude of the swing will decay over time. The hydrodynamics parameters can then be extracted from the time history of the motion. As the scaled model is allowed to oscillate freely in the water tank, the experiment is classified as a free decay test. By applying the laws of Similitude, the hydrodynamics parameters of the scaled model can be scaled up to predict the corresponding values for the full scale vehicle. Then, verification is performed by comparing the experimental values obtained with that predicted by CFD for the full scale ROV.

The proposed method has few advantages. Firstly, the motion of the pendulum is restricted in a plane and has only one DOF. The position of pendulum is fully described by variable θ. The motion is appropriately constrained and hence, the dynamics equation of motion could represent the motion correctly. Therefore, the result will be more accurate. Secondly, the variable θ can be measured easily using a potentiometer or an encoder. However, in this experiment, the angle θ is obtained through visual sensing using a digital camera. The method is very simple and reasonably accurate. As a whole, the experimental setup is simple and is very low cost compared with the building cost of a water tunnel facility with PMM equipment.
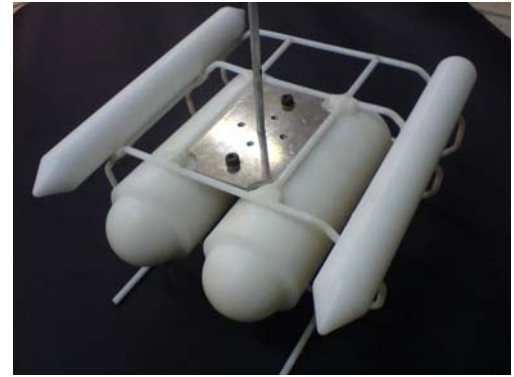
Fig. 1. The scaled down model of the ROV II.

II. THEORY

A. Nomenclature

TABLE I: Nomenclature

M	Mass of the scaled Model
m_a	Added Mass in single DOF
g	Gravity term
B	Buoyancy
θ	Angle of rotation of the pendulum
r	Length of the pendulum (radius)
K_L	Linear Damping Coefficient
K_Q	Quadratic Damping Coefficient
F_{rod}	Tension Force from the rod
F_H	Hydrodynamics Force
v	Tangential Velocity

B. Dynamics Equation

Consider an object of interest attached at the end of the pendulum and fully submerged in the water. The object moves in a circular path with radius r as shown in Fig 2. In the earth-fixed frame, the object is rotating about the pivot point. However, in the body-fixed frame, the object only moves in the surge direction at any instant; the object has only velocity component in surge direction.
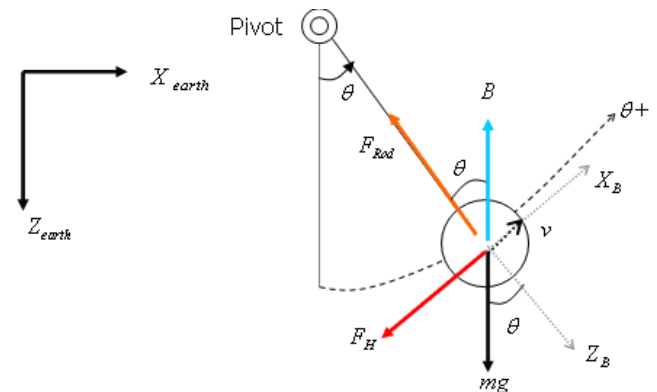
Fig. 2. Free Body Diagram of the Pendulum under Hydrodynamics Forces

The added mass and damping coefficient are defined in body fix frame such that,

$$F_H = m_a \ddot{x} + K_L \dot{x} + K_Q |\dot{x}| \dot{x} \qquad (1)$$

The equation of motion in the surge direction using Newton's second law of motion:

$$\sum F_x = M\ddot{x}$$

$$-Mg\sin\theta + B\sin\theta - m_a\ddot{x} - K_L\dot{x} - K_Q|\dot{x}|\dot{x} = M\ddot{x} \qquad (2)$$

Rearranging equation (2) gives:

$$(B - Mg)\sin\theta - K_L\dot{x} - K_Q|\dot{x}|\dot{x} = (M + m_a)\ddot{x}$$

$$\ddot{x} = \frac{(B - Mg)}{(M + m_a)}\sin\theta - \frac{K_L}{(M + m_a)}\dot{x} - \frac{K_Q}{(M + m_a)}|\dot{x}|\dot{x}$$

$$\qquad (3)$$

For rotational motion, $\dot{x} = r\dot{\theta}$ and $\ddot{x} = r\ddot{\theta}$

$$r\ddot{\theta} = \frac{(B - Mg)}{(M + m_a)}\sin\theta - \frac{K_L}{(M + m_a)}r\dot{\theta} - \frac{K_Q}{(M + m_a)}|r\dot{\theta}|r\dot{\theta}$$

$$\ddot{\theta} = \frac{(B - Mg)}{(M + m_a)r}\sin\theta - \frac{K_L}{(M + m_a)}\dot{\theta} - \frac{K_Q \cdot r}{(M + m_a)}|\dot{\theta}|\dot{\theta}$$

Let $\alpha = \dfrac{(B - Mg)}{(M + m_a)r}$, $\beta = \dfrac{K_L}{(M + m_a)}$ and $\gamma = \dfrac{K_Q \cdot r}{(M + m_a)}$

Then $\ddot{\theta} = \alpha \cdot \sin\theta - \beta \cdot \dot{\theta} - \gamma \cdot |\dot{\theta}|\dot{\theta} \qquad (4)$

C. Least Square

Using least square method [11] to obtain the estimated α, β, γ

$$\begin{bmatrix} \ddot{\theta}_1 \\ \ddot{\theta}_2 \\ \vdots \end{bmatrix} = \begin{bmatrix} \sin\theta_1 & \dot{\theta}_1 & |\dot{\theta}_1|\dot{\theta}_1 \\ \sin\theta_2 & \dot{\theta}_2 & |\dot{\theta}_2|\dot{\theta}_2 \\ \vdots & \vdots & \vdots \end{bmatrix} \begin{bmatrix} \alpha \\ \beta \\ \gamma \end{bmatrix} + error \qquad (5)$$

$$\underbrace{}_{y} \quad \underbrace{}_{H(x)} \quad \underbrace{}_{\theta}$$

Subscript i = 1, 2, 3... represents the number of samples collected from the experiment

Result, $\hat{\theta}_{LS} = (H^T H)^{-1} H^T y \qquad (6)$

Standard deviation, $\hat{\sigma}_\theta = \sqrt{diag\left(\text{cov}(\hat{\theta}_{LS})\right)}$

where $\text{cov}(\hat{\theta}_{LS}) = \hat{\sigma}^2 (H^T H)^{-1} \qquad (7)$

D. Similitude Law

Similitude Law states that two different systems with similarity in behavior will have equal similarity in parameters. In other words, if the flow patterns for two different systems are similar, it is possible to predict the parameters for the real model using the data from the scaled model.

Drag Coefficient Vs Reynolds Number
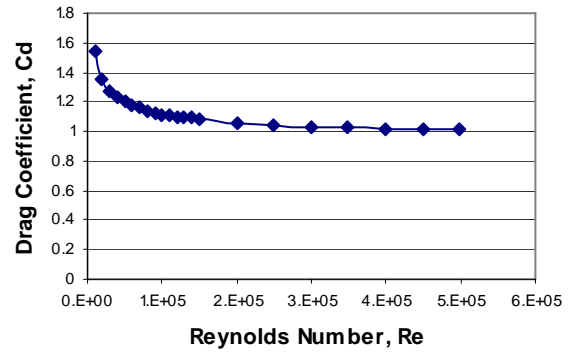
Fig. 3. Drag Coefficient versus Reynolds Number

From dimensional analysis and by using the Buckingham π theorem, the drag force acting on a submerged object is:

$$D = \frac{1}{2}\rho C_d A V^2 \qquad (8)$$

where D = Drag Force; ρ = fluid density; A = frontal area; V = velocity and C_d = drag coefficient

From [12], the drag coefficient for a submerged object is a function of Reynolds Number. So, the similitude is satisfied by having the same Reynolds Number for the two flows. Since water is used as the working fluid for both cases, the density and viscosity are identical. In order to have the same drag coefficient, the model must move at about three times faster than the real model. However, a CFD study for the operating range of flow speeds (0-0.5m/s) has shown that the drag coefficients are nearly constant for the corresponding range of Reynolds Numbers as shown in Fig 3. From equation (8), the ratio of drag force experienced by the real model to the drag force experienced by the scaled model at the same speed is:

$$\frac{D_t}{D_m} = \frac{\frac{1}{2}\rho C_d A_t V^2}{\frac{1}{2}\rho C_d A_m V^2} = \frac{A_t}{A_m} = \left(\frac{L_t}{L_m}\right)^2 = \left(\frac{1}{0.3}\right)^2 = 11.111 \qquad (9)$$

For rotational drag [13],

$$T_d = \sum_i r_i f_{di}$$

$$= \sum_i r_i \left(\frac{1}{2}C_d \rho A_{pi} r_i^2 \dot{\theta}^2\right) = C_D \rho A_p L^3 \dot{\theta}^2$$

$$\frac{T_t}{T_m} = \frac{C_D \rho A_{pt} L_t^3 \dot{\theta}^2}{C_D \rho A_{pm} L_m^3 \dot{\theta}^2} = \frac{A_{pt} L_t^3}{A_{pm} L_m^3} = \left(\frac{L_t}{L_m}\right)^5 = \left(\frac{1}{0.3}\right)^5 = 411.52 \qquad (10)$$

For the added mass coefficients, the scaling factor from scaled model to real ROV II can be obtained from [14].

III. EXPERIMENT

The experimental setup is simple and the costs involved are minimal. The setup is shown in Fig 4. A scaled *model* of the ROV is attached to one end of a pendulum in the water. A transparent water tank (1mx2mx1m) was used so that the motion can be captured by a digital camera. A hanging scale is used to measure the weight of the scaled model.
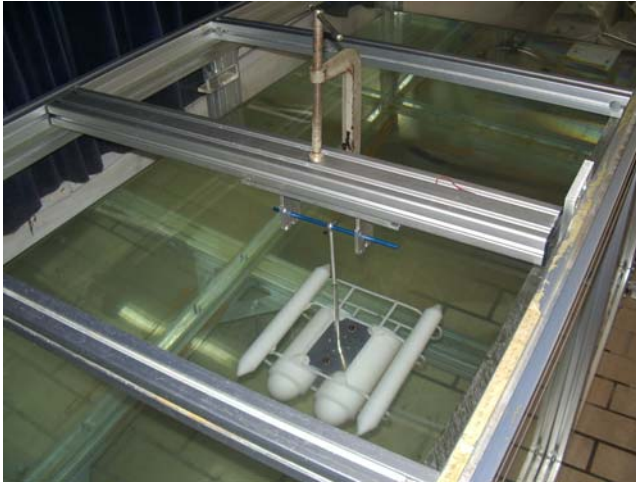
Fig. 4. Experimental Setup

Experimental Procedure

First, put a small black mark on the rod. Next, attach the fixture to the structure of the water tank with a G-clamp as shown in Fig 4. Set the camera up to capture the trajectory of the black mark when pendulum is swinging. The black mark must distinguish itself from its background for ease of image processing. After that, displace the pendulum from its equilibrium, up to approximate 45 degrees and then release it to swing freely in the water. Record the trajectory of the black mark using the video camera. Then, download the recorded video into PC and split the video into a number of frames using a open-source program *VirtualDubMod* [15]. For each frame, the x and y coordinates of the black mark are acquired using image processing method. In this project, MATLAB[TM] Image Processing Toolbox had been used to write a program script to automate the localization of the marker. Next, the time history of θ is determined from the x and y coordinates using equation 6. Finally, apply the least square algorithm to calculate the added mass, linear damping and quadratic damping (m_a, K_L, K_Q).

IV. EXPERIMENT RESULT & DISCUSSION

The experiment described in the preceding paragraph is being conducted in 2 different mediums (air and water)

A. In Air

The objectives to conduct experiments in air are to verify the feasibility of the method by comparing the pendulum length calculated from experimental data and pendulum length measured by ruler and to determine the friction at the pivoting point by calculating the linear and quadratic damping in air.

From each image frame, the *x* and *y* coordinates of the black marker is found. The center of rotation (about the pivot point) is found by fitting the arc on the *x* and *y* coordinates as shown in Fig 5.
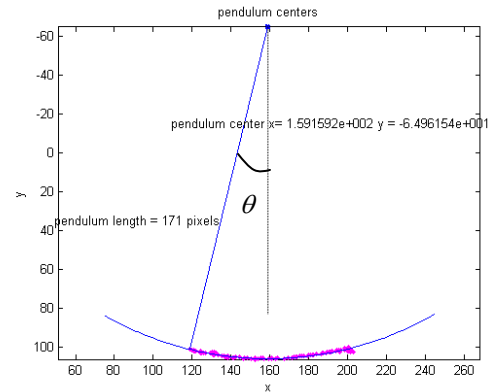
Fig. 5. Plot of the coordinate of the marker in the image sequences.

$$\theta = \tan^{-1}\left(\frac{x_i - x_{center}}{y_i - y_{center}}\right) \quad (11)$$

Since the experiment was conducted in air, the buoyancy B and added mass are negligible.

From the least square algorithm:

$$\alpha = \frac{B - Mg}{(M + m_a)r} = -25.1280 \Rightarrow r = 0.3904m$$

$$\beta = \frac{-K_L}{(M + m_a)} = 0.0260 \Rightarrow K_L = -0.0079N/ms^{-1}$$

From measurement, *r* is 0.39m

$$\gamma = \frac{-K_Q r}{(M + m_a)} = -0.0481 \Rightarrow K_Q = 0.0057N/(ms^{-1})^2$$
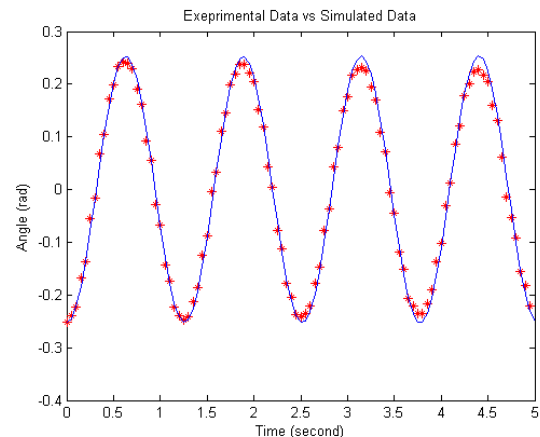
Fig. 6. Experimental data versus simulated data in air
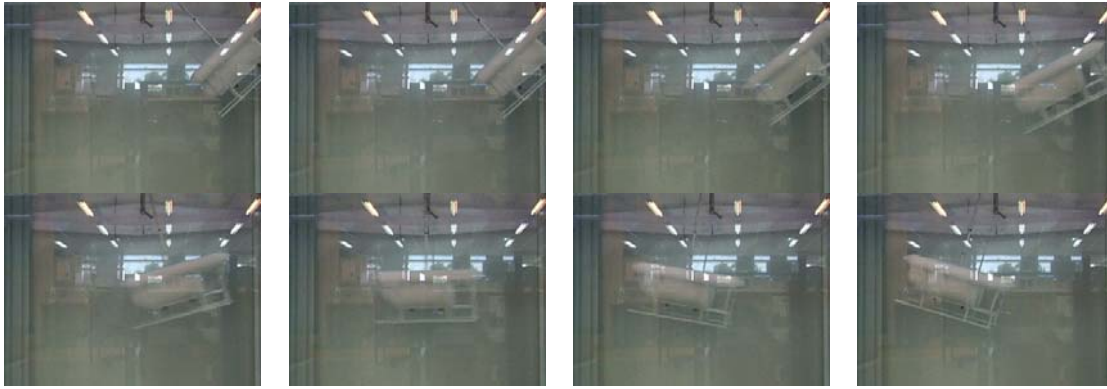
Fig. 7. Image Sequence of the *scaled* model under pendulum motion

Fig 6 shows the experimental data versus simulated data generated by a Simulink^{TM} model. The pendulum performs a near simple harmonic motion, which could be described by a sinusoidal function. The amplitude decay is small showing that the friction at pivoting point is negligible. The simulation model is able to capture the motion of the pendulum with a reasonable degree of accuracy. This means that proposed method is feasible and reliable.

B. In Water

The experiment is now repeated in water. First, the buoyancy of the vehicle needs to be determined by measuring the weight of the fully submerged model using a force sensor. A camera is used to record the pendulum motion and the video is split into multiple frames up to 30 frames per second. Fig 7 illustrates the free decay motion of the pendulum by showing some image frames.

Three experiments have been conducted in the surge directions. The results obtained are tabulated in Table II. The root mean square (RMS) of the error is also calculated. The error is defined as the difference between the simulated result and experimental result. Despite the simple experiment setup, the result obtained is highly repeatable and consistent. The RMS of the error of each test is around 0.05 radians. The small value of the RMS error is expected since it is evidence in Fig 8, that the simulated data match closely the experimental data.

The same method is used to identify the hydrodynamics coefficients in the sway and heave directions. The results are not shown here due to space limit. Beside the surge, sway and heave, the hydrodynamics coefficient for yaw motion is equally important. In order to identify the coefficients in the yaw motion, the pendulum's rod is replaced by a torsion spring. The scaled model will exhibit pure rotational motion in the water. The dynamics equation needs to be changed to:

$$\ddot{\theta} = \frac{K}{(I+I_a)}\theta - \frac{K_L}{(I+I_a)}\dot{\theta} - \frac{K_Q}{(I+I_a)}\left|\dot{\theta}\right|\dot{\theta} \qquad (12)$$

where K, Torsion Spring constant

K_L, Linear Rotational Drag coefficient

K_Q, Quadratic Rotational Drag coefficient

I_a, Added Moment of Inertia

θ, Angle Theta

TABLE II: Result for three tests in surge direction

SURGE	Maximum Speed	0.55m/s		
test	Added-Mass (Kg)	Linear Damping (N/(ms^{-1}))	Quad Damping (N/(ms^{-1})^2)	RMS Error (radian)
1	0.5581	1.2736	9.9392	0.0568
2	0.6054	1.7768	9.1907	0.0470
3	0.5765	1.6040	9.5018	0.0552
Average	0.5800	1.5515	9.5439	0.0530
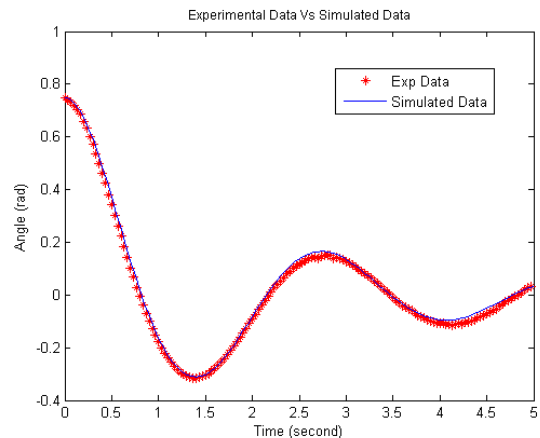
Fig. 8. Experiment data versus simulated data for angle θ in surge direction

C. Comparison with CFD

The experimental results determined from the free decay test of the scaled model are scaled up to the size of the ROV using the similitude's law discussed in Section 2D. These values are then compared with simulation results of the real vehicle using commercial computational fluid dynamics (CFD) program such as WAMIT and ANSYS CFX. It is observed that the calculated added masses from WAMIT closely match that with the experimental values in

surge, sway, heave, and yaw in Table III.

For hydrodynamics drag, comparison should not be done on the basis of K_L versus K_L or K_Q versus K_Q as shown in Table IV. Instead, the combination effect of both should be compared by plotting the total drag force against the velocity range of operation as shown in Fig 9 and 10. The results agree well with the result obtained from ANSYS CFX.

TABLE III: Comparison of Added Mass Coefficients

	Surge	Sway	Heave	Yaw
Experiment	21.42	55.01	113.33	3.60
WAMIT	19.63	51.75	104.12	3.97

TABLE IV: Comparison of Hydrodynamics Drag Coefficients

Direction Range	Surge (0-0.5m/s)		Yaw (0-0.52rad/s)	
Parameter	K_L	K_Q	K_L	K_Q
Experiment	17.24	106.03	1.18	7.51
ANSYS CFX	11.86	108.45	0	10.39

Surge Drag vs Velocity
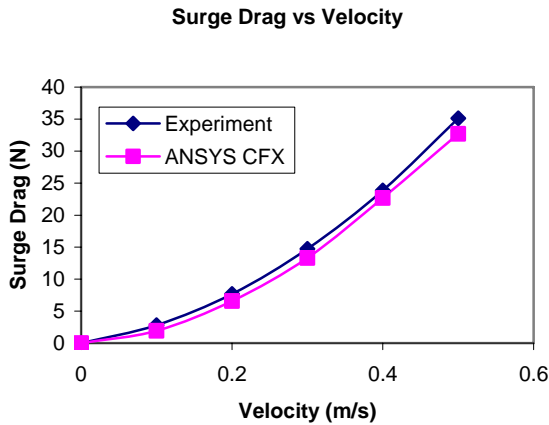
Fig. 9. Drag in surge direction.

Yaw Drag vs Angular Velocity
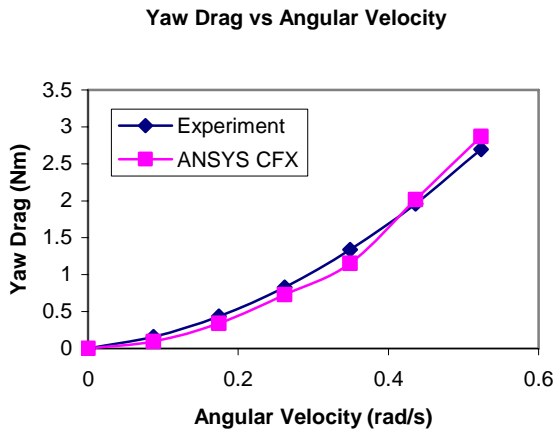
Fig. 10. Drag in yaw direction

V. CONCLUSION

A new free decay test has been proposed to identify the added mass and drag coefficient of a scaled down model of the ROV II. The test makes use of the pendulum swing motion to identify coefficients in surge, sway and heave and a torsion pendulum motion to identify coefficients in yaw. Although the experiment setup is very simple and low cost, the result obtained is reasonably reliable. The result can be scaled up to predict the coefficients for ROV II.

REFERENCES

[1] G. Bekey, R. Ambrose, V. Kumar, A. Sanderson, B. Wilcox, and Y. Zheng, "International Assessment of Research and Development in Robotics," World Technology Evaluation Center, Inc. 2006.

[2] M. Caccia, G. Indiveri, and G. Veruggio, "Modeling and identification of open-frame variable configuration unmanned underwater vehicles," *IEEE Journal of Oceanic Engineering*, vol. 25, pp. 227-240, 2000.

[3] A. Alessandri, R. Bono, M. Caccia, G. Indiveri, and G. Veruggio, "Experiences on the modelling and identification of the heave motion of an open-frame UUV," presented at Oceans Conference Record (IEEE), Nice, Fr, 1998.

[4] A. T. Morrison, III and D. R. Yoerger, "Determination of the hydrodynamic parameters of an underwater vehicle during small scale, nonuniform, 1-dimensional translation," Victoria, BC, Canada, 1993.

[5] [5] G. Conte, S. M. Zanoli, D. Scaradozzi, and A. Conti, "Evaluation of hydrodynamics parameters of a UUV. A preliminary study," presented at International Symposium on Control, Communications and Signal Processing, ISCCSP, Hammamet, 2004.

[6] P. Egeskov, A. Bjerrum, A. Pascoal, C. Silvestre, C. Aage, and L. W. Smitt, "Design, construction and hydrodynamic testing of the AUV MARIUS," Cambridge, MA, USA, 1994.

[7] C. Aage and L. Wagner Smitt, "Hydrodynamic manoeuvrability data of a flatfish type AUV," Brest, France, 1994.

[8] [8] P. Ridao, A. Tiano, A. El-Fakdi, M. Carreras, and A. Zirilli, "On the identification of non-linear models of unmanned underwater vehicles," *Control Engineering Practice*, vol. 12, pp. 1483-1499, 2004.

[9] [9] D. A. Smallwood and L. L. Whitcomb, "Adaptive identification of dynamically positioned underwater robotic vehicles," *IEEE Transactions on Control Systems Technology*, vol. 11, pp. 505-515, 2003.

[10] T. I. F. A. Ross, and T. A. Johansen, "Identification of underwater vehicle hydrodynamic coefficients using free decay tests," *IFAC Conference on Control Applications in Marine Systems, Ancona, Italy*, 2004.

[11] L. Ljung, *System identification: Theory for the user*: Englewoods Clifts, NJ: Prentice Hall., 1987.

[12] Munson, Young, and Okiishi, *Fundamentals of Fluid Mechanics, 5th Edition*: Wiley Higher Education.

[13] R.-C. C. T.-L. L. Chen-Chou Lin, "Experimental determination of the hydrodynamic coefficients of an underwater manipulator," *Journal of Robotic Systems*, vol. 16, pp. 329-338, 1999.

[14] M. S. Triantafyllou and F. S. Hover, *Manoeuvring and Control of Marine Vessels*: Department of Ocean Engineering, MIT, Cambridge, Massachusetts, USA, 2003.

[15] A. Lee, "VirtualDubMod," 2007.